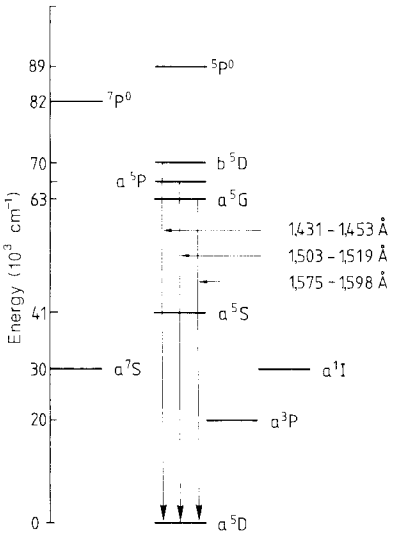

Fig. 2 A partial term scheme for Fe III, showing the observed transitions, some lower-lying terms of the same even parity and the first two terms of odd parity. Term energies are given in cm^{-1}.

abilities found by Garstang[8] for lower-lying levels are in each case ~1. Thus it is likely that the upper levels have populations close to their Boltzmann values with collisional de-excitation rates exceeding radiative decay rates. Then the ratio of the [Fe III] line fluxes to those of permitted transitions would be sensitive to the electron density. Detailed calculations of the atomic data are required to establish the collisional-radiative regime for the individual lines. The upper levels may attain only a pseudo-Boltzmann population if collisional excitation to higher states of odd parity exceeds the rate for collisional de-excitation to lower levels. In any case the new [Fe III] identifications will provide more information on the structure of the solar chromosphere-corona transition region.

If the a^5G, a^5P and b^5D levels are collisionally de-excited in the solar atmosphere, they could become stronger, relative to permitted transitions of species of similar excitation, in astrophysical sources of lower electron density. For this reason their presence is being investigated in such sources, including the Seyfert galaxy NGC 4151, which has unidentified emission features around 1,575, 1,581 and 1,518 Å (refs 13 and 14). [Fe III] emission is observed in the optical spectrum of NGC 4151[15,16]. The relative intensities of the quintet transitions in NGC 4151 and other sources cannot be predicted until collision cross-sections and transition probabilities are known, and these are urgently required to establish whether or not the [Fe III] lines are of wider astrophysical significance.

Received 3 September; accepted 23 October 1986.

1. Bartoe, J.-D. F., Brueckner, G. E., Purcell, J. D. & Tousey, R. *Appl. Opt.* **16**, 879–885 (1977).
2. Sandlin, G. D., Bartoe, J.-D. F., Brueckner, G. E., Tousey, R. & VanHoosier, M. E. *Astrophys. J. suppl. Ser.* **61**, 801–898 (1986).
3. Jordan, C., Brueckner, G. E., Bartoe, J.-D. F., Sandlin, G. D. & VanHoosier, M. E. *Astrophys. J.* **226**, 687–697 (1978).
4. Bartoe, J.-D. F. *et al.* in *AIAA 24th Aeropsace Sciences Meeting, Reno*, AIAA-86-0225 (in the press).
5. Moore, C. E. in *Selected Tables of Atomic Spectra: Atomic Energy Levels and Multiplet Tables, Si I.* NSRDS-NBS-3, Sect. 2 (1967).
6. Edlén, B. & Swings, P. *Astrophys. J.* **95**, 532–554 (1942).
7. Reader, J. & Sugar, J. *J. phys. chem. Ref. Data* **4**, 353–440 (1975).
8. Garstang, R. H. *Mon. Not. R. astr. Soc.* **117**, 393–405 (1957).
9. Garstang, R. H., Robb, W. D. & Rountree, S. P. *Astrophys. J.* **222**, 384–397 (1978).
10. Abbott, D. C. *J. Phys.* **B11**, 3479–3497 (1978).
11. House, L. L. *Astrophys. J. suppl. Ser.* **8**, 307–328 (1964).
12. Munro, R. H. & Withbroe, G. L. *Astrophys. J.* **176**, 511–520 (1972).
13. Ulrich, M. H. *et al. Nature* **313**, 747–751 (1985).
14. Cassatella, A. & Jordan, C. (in preparation).
15. Boksenberg, A. *et al. Mon. Not. R. astr. Soc.* **173**, 381–386 (1975).
16. Boksenberg, A. & Penston, M. V. *Mon. Not. R. astr. Soc.* **177**, 127P–131P (1976).

A hierarchical $O(N \log N)$ force-calculation algorithm

Josh Barnes & Piet Hut

The Institute for Advanced Study, School of Natural Sciences, Princeton, New Jersey 08540, USA

Until recently the gravitational N-body problem has been modelled numerically either by direct integration, in which the computation needed increases as N^2, or by an iterative potential method in which the number of operations grows as N log N. Here we describe a novel method of directly calculating the force on N bodies that grows only as N log N. The technique uses a tree-structured hierarchical subdivision of space into cubic cells, each of which is recursively divided into eight subcells whenever more than one particle is found to occupy the same cell. This tree is constructed anew at every time step, avoiding ambiguity and tangling. Advantages over potential-solving codes are: accurate local interactions; freedom from geometrical assumptions and restrictions; and applicability to a wide class of systems, including (proto-)planetary, stellar, galactic and cosmological ones. Advantages over previous hierarchical tree-codes include simplicity and the possibility of rigorous analysis of error. Although we concentrate here on stellar dynamical applications, our techniques of efficiently handling a large number of long-range interactions and concentrating computational effort where most needed have potential applications in other areas of astrophysics as well.

Until recently, the dynamics of a system of self-gravitating bodies (the gravitational N-body problem) has been modelled numerically in two fundamentally different ways. The first one, direct N-body integration, involves the computation of all $\frac{1}{2}N(N-1)$ forces between all pairs of particles. This allows an accurate description of the dynamical evolution but at a price that grows rapidly for increasing N[1]. The second way involves a two-step approach: after fitting the global potential field to a special model with a number of free parameters, each particle is propagated in this background field for a short time before the same procedure is reiterated. The potential method involves a number of operations that grow only as N log N. Thus calculations can be performed more quickly, but with a loss of accuracy and generality. The special nature of each potential-solving code is caused by the need to use some technique that is tuned to the geometry of the problem being considered (such as Fourier transforms or spherical or bispherical harmonics[2]).

Recently, some of the advantages of both approaches have been combined by using direct integrations of force while grouping together increasingly large groups of particles at increasingly large distances. This corresponds to the way humans interact with neighbouring individuals, further villages and increasingly further and larger states and countries—driven by increasing cost and decreasing need to deal with more removed groups on an individual basis. The first implementation of such a hierarchical grouping of interactions was given by Appel[3], who used a tree structure to represent an N-body system, with the particles stored in the leaves of the tree. An independent implementation by Jernigan[4] and Porter[5] incorporated regularization of close encounters. However, in both codes the logarithmic-growth gain in efficiency comes at the price of introducing additional errors that are hard to analyse because of the arbitrary structure of the tree. Nearby particles may be grouped as leaves of nearby branches, but the phase-space flow of realistic self-gravitating systems demands a continuous updating of the tree structure to avoid tangling and unphysical grouping, requiring complicated book-keeping. It is not at all clear how to understand and estimate the errors caused by the process of approximating lumps of particles together as single pseudo-particles, because individual lumps can take more or less arbitrary shapes and sizes.

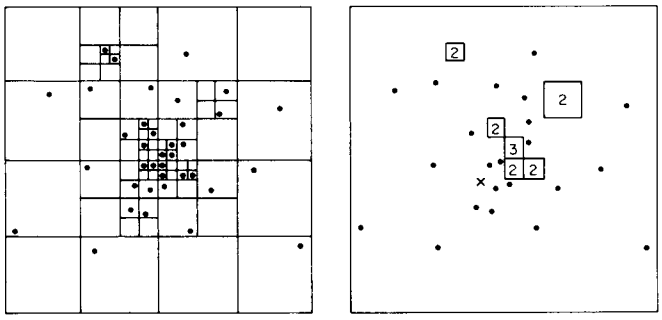

Fig. 1 Hierarchical boxing and force calculation, presented for simplicity in two dimensions. On the left, a system of particles and the recursive subdivision of system space induced by these particles. Our algorithm makes the minimum number of subdivisions necessary to isolate each particle. On the right, how the force on particle x is calculated. Fitted cells contain particles that have been lumped together by our 'opening angle' criterion; each such cell represents a single term in the force summation.

We present here a new way of realizing a tree-based force calculation with logarithmic growth of force terms per particle that avoids the tree-tangling complications mentioned above, allows rigorous upper bounds for errors that arise from neglecting internal lump structure, and also offers a well-defined procedure for estimating more typical, average errors. The essential ingredients are (1) a virtual cubical division of empty space in (sub)cells with daughter cells having exactly half the length, breadth and width of their parent; (2) the construction of the actual tree of cells from the virtual one by (i) discarding empty subcells, (ii) accepting subcells with one occupant, and (iii) recursively dividing shared occupancies in sub-subcells; and (3) performing this reconstruction *ab initio* at every time step.

Given this book-keeping structure, the dynamics are implemented by assigning to every non-empty cell, as well as to higher-order cells containing more than one particle, a (pseudo-)particle that contains the total mass in the cell located at the centre-of-mass of all the particles it contains. Any single real particle feels the force of all (pseudo-)particles in the system that represent a cell small enough and far enough to forego the need of further division, thereby screening all its component (pseudo-)particles.

A computer program that implements the hierarchical force calculation is available from us upon request. It contains less than a thousand lines of C code: 150 lines of definitions, 150 lines for tree construction, 100 lines for force calculation and 100 lines for a simple integrator; the remaining lines handle input-output book-keeping.

In what follows we summarize some of the more technical details. The method we use to compute a force in time of $O(\log N)$ is based on a representation of the mass distribution as a hierarchical tree structure, constructed as follows. Begin with an empty cubical cell big enough to contain the system. One by one, load particles into this 'root' cell. If any two particles fall into the same cell, divide that cell into eight cubical subcells (thus the first such division occurs as soon as the second particle has been loaded in, splitting the system into at least eight pieces). Each divided cell is represented by a data structure that holds information about the subcells it contains: a summary of global physical quantities (mass and centre-of-mass position) as well as pointers to the daughter cells, which may be referenced to obtain more detailed information. Continue this process of subdividing to as high a level as required. When all N particles have been loaded, the system space will have been partitioned up into a number of cubical cells of different sizes, with at most one particle per cell. These particle-bearing cells are grouped together into larger cubical cells, which are grouped together into still larger parent cells, and so on down to the root cell, which contains the entire system. The average size of a particle-bearing cell is of the order of the interparticle spacing, so the 'height of the tree' (that is, the number of subdivisions required to reach a typical cell, starting at the root), is of $O(\log_2 N^{1/3}) = O(\log N)$, and the time required to construct the tree is of $O(N \log N)$. The final step in constructing the tree is to tag the subdivided cells with the total mass and centre-of-mass position of the particles they contain; by propagating information down the tree from the particles towards the root, this step may also be accomplished in a time of $O(N \log N)$.

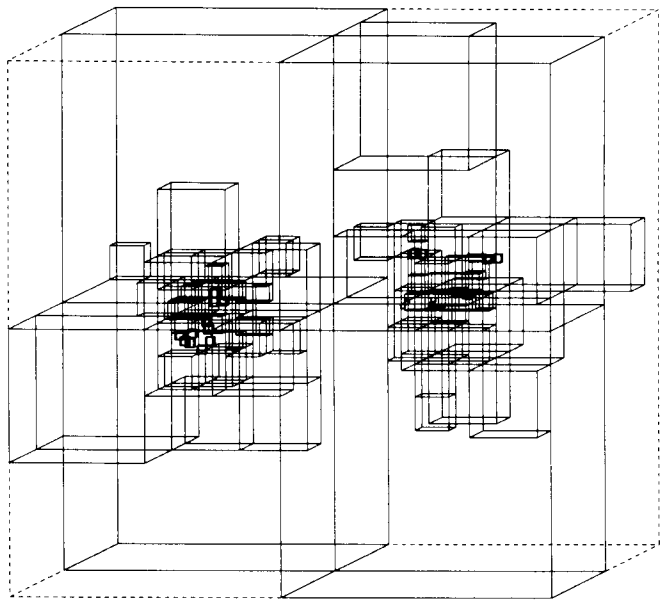

Fig. 2 Box structure induced by a three-dimensional particle distribution. This example was taken from the early stages of an encounter of two $N = 64$ systems, and shows how the boxing algorithm can accommodate systems with arbitrarily complicated geometry. The particle distribution corresponding to a system with 32 times as many members is shown in Fig. 3.

Having constructed such a tree, the force on any particle p may be approximated by a simple recursive calculation. Start at the root cell of the tree, which contains the entire system. Let l be the length of the cell currently being processed and D the distance from the cell's centre-of-mass to p. If $l/D < \theta$, where θ is a fixed accuracy parameter ~ 1, then include the interaction between this cell and p in the total being accumulated. Otherwise, resolve the current cell into its eight subcells, and recursively examine each one in turn. The core of the force calculation routine may be compactly expressed in SCHEME, a dialect of LISP:

```
(define (acceleration particle ensemble)
  (cond ((singleton? ensemble)
         (newton-acceleration particle (the-element ensemble)))
        ((< (/ (diameter ensemble)
               (distance particle (centroid ensemble)))
           theta)
         (newton-acceleration particle (centroid ensemble)))
        (else
         (reduce sum-vector
                 (map (lambda (e) (acceleration particle e))
                      (subdivisions ensemble))))))
```

Note that in LISP, a function with arguments $f(x, y, \ldots)$ is written as $(f\ x\ y \ldots)$. For example, (newton-acceleration p_1 p_2) calls a function to compute the acceleration of particle p_1 due to p_2. The (cond ...) form is a three-way conditional, computing the acceleration directly in the first two cases, and by recursion in the final (else ...) clause. Elements of the SCHEME programming language are presented in Abelson *et al.*[6]. Figure 1

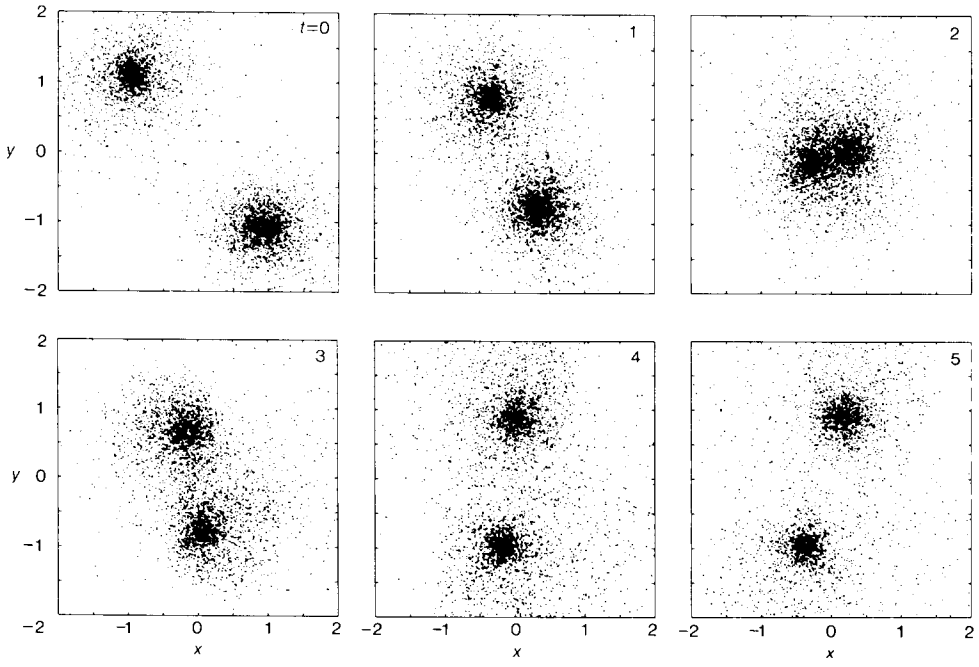

Fig. 3 Encounter of two spherical systems, simulated by using our hierarchical acceleration technique in combination with a simple leap-frog integrator. The incoming systems were launched on parabolic orbits, but become bound because of dynamical friction. Note the striking wakes lagging behind the density centres of the two systems at $t = 3$, 4 (in our units the gravitational constant, the mass of each galaxy and the total binding energy of the whole system all equal unity). With a total of $N = 4{,}096$ particles in the system and an opening angle criterion of $\theta = 1$, the number of two-body interactions computed by our technique is less than 0.1 of the $\frac{1}{2}N/(N-1)$ required by a direct-summation force calculation. The calculation took 10 h on a VAX 11/780 (in double precision because of compiler limitations; a single-precision calculation would take half as long). With a time step $\Delta t = 0.05$ and softening parameter $\varepsilon = 0.025$, energy was conserved to ~1%.

illustrates this process for a small number of particles in two dimensions; increasing the number to $10^4 \sim 10^5$ in three dimensions typically increases the number of interactions per particle to only of order 10^2.

The number of interactions considered by this procedure in computing the force on p is of order log N for large N. Suppose the mass distribution is homogeneous within the root cell. Increasing the total number of particles eightfold is roughly equivalent to adjoining eight similar root cells together. The seven new cells not containing p will contribute some 'relatively small' number ΔN_t of additional terms to the force approximation. Now the expectation value $\langle \Delta N_t \rangle$ depends on θ, but not on the total number of particles or the size of the system. Thus the time required to calculate the force on a particle increases by a constant increment (of $\langle \Delta N_t \rangle$), whereas N increases by a constant factor (of eight). In other words, the time required by the CPU (central processing unit) to compute the force on a single particle is on the scale of $O(\log N)$.

A rigorous error analysis of the force-calculation algorithm is possible because our prescription yields a unique, well-characterized tree structure based on up-to-date particle positions. Each compound cell that we choose not to subdivide introduces a small error due to quadrupole and higher-order moments of the mass distribution within the cell (the dipole term vanishes when expanding around the centroid). The magnitude of this error may be bounded by a 'worst-case' analysis for which the quadrupole moment is maximized (for example, two lumps placed in opposite corners of the cell), and estimated from an analysis of root-mean-square fluctuations within each cell together with estimates of the coherence time scales for these fluctuations. We shall present this analysis in a more detailed paper. In practice, forces computed even with an opening angle parameter as large as $\theta = 1$ are still accurate to ~1% with little dependence on N. Empirically, we find the force error scales approximately as the −1.5 power of the computing time. These errors are only weakly correlated from one time step to the next, resulting in a build-up close to a random walk rather than a steady drift.

As a test of our new method, we have written a simple N-body code using our force-calculation scheme with a time-centred leap-frog integrator, in which positions and velocities are alternately advanced. A parabolic encounter of two galaxies is initiated at a distance of several galactic radii, leading to a box structure as shown in Fig. 2. The results of a 4096-body calculation of such an encounter are shown in Fig. 3. This calculation took 10 h of CPU time on a VAX 11/780 with a floating point accelerator.

There are several ways in which the code can be made more efficient. We are now investigating these, and we shall discuss our results in detail elsewhere. We just mention three possible improvements: (1) using a higher-order integration scheme such as Aarseth's fourth-order polynomial method rather than our second-order leap-frog method, which will require careful adjustments to avoid glitches caused by discrete differences between the grouping of particles in cells from one time step to the next (for example by multiply covering space in partly overlapping virtual grids); (2) including quadrupole moments in the description of cells as pseudoparticles characterized by the total mass in the cell as located in the centre of mass; (3) introducing individual time steps for particles which undergo strongly changing interactions, which could be accomplished by subsequently halving the time step when needed—thus extending the three-dimensional spatial halving of cells to a four-dimensional space-time division in rectangular subcells.

An interesting aspect of our new code is the different emphasis it places both on software and hardware, in comparison with other codes. On the hardware side, the hierarchical structure of our code does not lend itself easily to vectorization (although this may well be worth exploring). In contrast, we expect our code to be most useful on computers with highly parallel architectures (with one processor per particle, computer time is reduced approximately by a factor of N). On the software side, the hierarchical decomposition of the problem is best realized by using recursive descriptions. Recursive function calls and other general control and data structures are not well supported or clearly represented in FORTRAN. This has led us to consider other programming languages such as C, PASCAL and LISP. Another advantage offered by these languages is that they permit a clarity of presentation of our ideas, which makes the underlying techniques available to other researchers. Of course, if a particular computer has a FORTRAN compiler which is an order of magnitude faster than other compilers, it makes sense to translate a version of our program into FORTRAN, trading clarity and modularity for efficiency.

Our application to N-body calculations is only one in a range of possibilities including the calculation of radiation fields (replacing particles with sources) and self-gravitating fluid flow (cell division being governed by the complexity of the local flow pattern). Thus our technique forms a general tool for simultaneously handling a large number of long-range interactions and for concentrating computing resources locally where most needed.

We thank John Bahcall, Jeremiah Ostriker and especially Gerald Sussman for interesting discussions. Part of this work was supported by the NSF through grant PHY-8217352; P.H. is an Alfred P. Sloan Foundation fellow.

Received 16 July; accepted 1 October 1986.

1. Aarseth, S. J. in *Multiple Time Scales* (ed. Brackbill, J. U. & Cohen, B. I.) 377–418 (Academic Press, New York, 1985).
2. Hockney, R. W. & Eastwood, J. W. *Computer Simulation using Particles* (McGraw-Hill, New York, 1981).
3. Appel, A. *SIAM J. Sci. statist. Comput.* **6**, 85–103 (1985).
4. Jernigan, J. G. *I.A.U. Symp.* **113**, 275–284.
5. Porter, D. thesis, Physics Dept, Univ. California, Berkeley (1985).
6. Abelson, H., Sussman, G. J. & Sussman, J. *Structure and Interpretation of Computer Programs* (MIT Press, Cambridge, Massachusetts, 1985).

The 400-km seismic discontinuity and the proportion of olivine in the Earth's upper mantle

Craig R. Bina & Bernard J. Wood

Department of Geological Sciences, Northwestern University, Evanston, Illinois 60201, USA

The 400-km seismic discontinuity has traditionally been ascribed to the isochemical transformation of α-olivine to the β-modified-spinel structure in a mantle of peridotitic bulk composition[1–6]. It has recently been proposed[7,8] that the observed seismic velocity increase at 400 km depth is too abrupt and too small to result from a phase change in olivine but instead requires that the transition zone be chemically distinct in bulk composition from the uppermost mantle. By requiring phase relations in the Mg_2SiO_4-Fe_2SiO_4 system to be internally consistent thermodynamically, we find that the α–β transition in olivine of mantle $(Mg_{0.9}Fe_{0.1})_2SiO_4$ composition is extremely sharp, occurring over a depth interval (isothermal) of ~6 km. The magnitude of the predicted velocity increase is in agreement with that observed seismically[9,10] if the transition zone is composed of ~60–70% olivine. Thus, our results indicate that seismic velocities across the 400-km discontinuity are consistent with a transition zone of homogeneous peridotitic composition and do not require chemical stratification.

The 400-km seismic discontinuity reflects a change in elastic properties of the mantle and has been attributed to a phase transformation of olivine to a spinel-like structure at high pressures[1]. Subsequent work has given rise to a generally accepted model in which the discontinuity is attributed to such an isochemical phase change in a mantle of homogeneous olivine-rich, or peridotitic, composition[2–6]. This model has the advantage of simplicity and can be tested experimentally.

Recently, it has been suggested[7,8] that a phase transition in olivine would produce a gradual velocity increase over an appreciable depth interval—rather than the abrupt increase observed seismically—and that the magnitude of the increase would be more than twice that actually observed. It was proposed that the seismic data require the transition zone to be chemically distinct in bulk composition from the uppermost mantle, with the transition zone consisting of a pyroxene-garnet rich 'piclogite' composition containing either 16%[7] or 30%[8] olivine. The 400-km discontinuity is ascribed to either a change in chemical composition from peridotite to underlying piclogite or—if this periodotite/piclogite boundary is referred to shallower depths—to the transformation of pyroxene to a garnet-like structure.

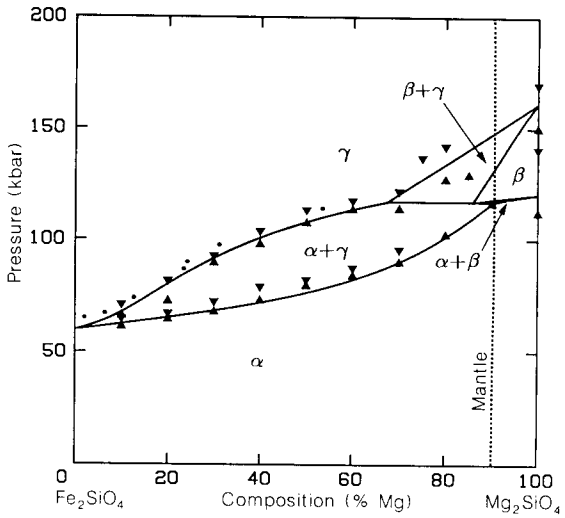

Fig. 1 Isothermal pressure-composition diagram showing calculated boundaries for olivine polymorph stability fields at 1,273 K. Also shown are experimental data points[12–14,18–20] delimiting the high-pressure stability limits of the low-pressure assemblages (▲), the low-pressure stability limits of the high-pressure assemblages (▼), and the compositions of γ phase which coexist with α phase at the indicated pressures (●). Dashed line shows $(Mg_{0.9}Fe_{0.1})_2SiO_4$ composition.

In a previous study[11], we showed that the transformation of pyroxene to a garnet structure would produce a smooth and gradual increase in seismic velocity, rather than the discontinuity observed at 400 km. In the present study, we have examined the olivine-spinel phase transitions to determine whether the observed seismic velocity variations may be attributable to such a phase change. The α-olivine to β-modified-spinel transition has been commonly represented by a broad '$\alpha+\beta$ divariant loop', a region in which both phases coexist in stable equilibrium. If this representation were accurate, the α phase would transform to the β phase in a continuous and gradual manner, and this phase change would not produce a sharp discontinuity in seismic velocity. However, the available experimental data (Fig. 1) do not constrain the width of this $\alpha+\beta$ loop, since no high-pressure experiments have yet produced both phases together in equilibrium for olivine of mantle $(Mg_{0.9}Fe_{0.1})_2SiO_4$ composition. We have used available thermoelastic and calorimetric data on the olivine polymorphs (α-olivine, β-modified-spinel, and γ-spinel) to constrain the width of the $\alpha+\beta$ divariant loop. By requiring the phase diagram for the Mg_2SiO_4-Fe_2SiO_4 system to be internally consistent thermodynamically, we have attempted to determine the sharpness and magnitude of a seismic discontinuity resulting from a phase change in olivine.

If the partial molar free energies of Mg_2SiO_4 and Fe_2SiO_4 components are known as functions of pressure, temperature, and composition, then the boundaries of the stability fields for the various phase assemblages (α, $\alpha+\beta$, β, $\beta+\gamma$ and so on) can be calculated explicitly. To compute the free-energy functions, we require knowledge of the enthalpies, entropies, volumes, and solution activities of the components in the various phases at the pressures, temperatures and compositions of interest. We used the available experimentally-measured values of the enthalpies and entropies[5,12–14], heat capacities[15], molar volumes and coefficients of thermal expansion[4], elastic moduli[16], and activity coefficients[17] for the phases and components in question. Where measured values were extremely uncertain or